Colloids and Surfaces B: Biointerfaces 90 (2012) 62–67

Contents lists available at SciVerse ScienceDirect

Colloids and Surfaces B: Biointerfaces

journal homepage: www.elsevier.com/locate/colsurfb

A amperometric biosensor for hydrogen peroxide by adsorption of horseradish peroxidase onto single-walled carbon nanotubes

Yanfeng Wang, Jie Du, Yaya Li, Duoliang Shan, Xibin Zhou, Zhonghua Xue, Xiaoquan Lu*

Key Laboratory of Bioelectrochemistry & Environmental Analysis of Gansu Province, College of Chemistry & Chemical Engineering, Northwest Normal University, Lanzhou 730070, PR China

ARTICLE INFO

Article history:
Received 16 June 2011
Received in revised form 17 August 2011
Accepted 27 September 2011
Available online 4 October 2011

Keywords:
Hydrogen peroxide
Horseradish peroxidase
Single-walled carbon nanotubes

ABSTRACT

Development of a highly sensitive nanostructured electrochemical biosensor based on the integrated assembly of horseradish peroxidase (HRP) and single-walled carbon nanotubes (SWNTs) is described. In this study, we describe the use of a sodium cholate suspension-dialysis method to adsorb the horseradish peroxidase (HRP) onto single-walled carbon nanotubes (SWNTs). We demonstrate that HRP–SWNTs conjugates can be assembled into amperometric biosensors which L-cysteine were assembled on a gold electrode through the covalent bond of S–Au and was used as a substrate for the immobilization of enzymes. Direct electron transfer of HRP is realized at SWNTs, and both anodic and cathodic currents of the redox reaction at the L-cysteine–HRP–SWNTs-modified gold film upon electrocatalysis are amplified. Meanwhile, experimental results reveal that HRP is stably immobilized onto the SWNTs and maintains inherent enzymatic activity toward H_2O_2. The modified electrode shows high sensitivity toward H_2O_2. A linear response to hydrogen peroxide measurement is obtained over the range from 1.0×10^{-12} to 1.0×10^{-11} M and an amperometric detection limit of 2.1×10^{-13} M due to its bioelectrocatalytic reduction based on direct electron transfer between gold electrode and the active site of the HRP. The biosensor displays excellent operational, storage stability and highly sensitive. The excellent performance validates the integrated assembly as an attractive sensing element for the development of a new hydrogen peroxide amperometric biosensor.

1. Introduction

Electrical communication between redox sites of enzyme and electrode is the basis for developing various amperometric biosensor devices [1]. Nevertheless, direct electron transfer is usually impossible with most enzymes because their redox centers are located deep inside the insulated protein shells. Therefore, some carbon materials, such as carbon nanotubes [2,3], carbon nanofibers [4], and highly ordered mesoporous carbons [5,6], are required in order to establish an electrical connection between these redox centers and the electrode [7] for fabricating a third-generation enzyme biosensor.

Single-walled carbon nanotubes (SWNTs) possess highly unique electronic, mechanical, and optical properties, making them the subject of intense study because of their discovery in 1993 by Iijima [8,9]. A large length-to-diameter ratio and a good conductivity of the SWNTs, make it possible to form a three-dimensional conducting matrix that can be used for immobilization of enzymes and proteins, more importantly, direct electron transfer of those biomacromolecules [10] enhanced faradaic responses [11]. However, As-synthesized single-walled carbon nanotubes (SWNTs) are bundled, preventing their efficient application [12]. To improve upon the properties of the SWNTs, low-cost and simple approaches utilizing a sodium cholate suspension-dialysis process to their debundled modification have been much pursued vigorously in recent times [13–15]. In this way, the proteins were adsorbed to form a stable solution-phase complex with SWNTs, neither the native structure and biological activity of proteins nor the unique propertie of SWNTs was lost.

The functionalized single-walled carbon nanotubes (SWNTs) are promising materials as carriers for enzyme immobilization [16,17]. The main advantage of using functionalized SWNTs is that the biomolecules can be immobilized firmly onto the SWNTs through covalent binding at the functional sites or noncovalent methods. Benefits of covalent immobilization are that it provides a strong linkage of the protein to the SWNTs and may increase the stability of the protein [18]. However, covalent coupling normally damages the sidewalls of SWNTs and disrupts their unique, electrical and optical properties [19–21]. In contrast, noncovalent methods can allow for the electronic structures and the geometric structures of the SWNTs [14,22–26] to be retained. Recently, a noncovalent method of protein attachment to SWNTs utilizing a sodium

* Corresponding author. Tel.: +86 931 7971276; fax: +86 931 7971323.
E-mail addresses: luxq@nwnu.edu.cn, taaluxq@126.com (X. Lu).

0927-7765/$ – see front matter.
doi:10.1016/j.colsurfb.2011.09.045

cholate suspension-dialysis process has been developed [13,14]. This method has been successful in coupling both the enzyme glucose oxidase [13] and horseradish peroxidase to SWNTs [14].

Among many different strategies used for the modification of electrode surfaces, the self-assembly technique exhibits unprecedented flexibility to tailor interfacial properties and presents biologically relevant groups, which makes it well-suited for the control of biomolecular density and orientation at the solid-liquid interface to obtain better reproducibility and higher efficiency [25]. It is well known that alkyl or aromatic disulfides and thiols form a close-packed ordered monolayer, "self-assembled monolayer" (SAM), on gold or silver surfaces via chemisorptive S–Au or S–Ag bonds [27–29]. The strength of this covalent bond is 40 kcal/mol [30]. Based on this principle, L-cysteine can form self-assembled monolayers on gold surfaces.

The direct electron transfer of immobilized proteins such as HRP [31], cytochrome C [32], and hemoglobin [33] with regard to Fe(III) to Fe(II) conversion has been well studied and extensively employed for biosensing and the preparation of mediator-free biosensors [34]. Direct electrical contacting of redox proteins to electrodes has been accomplished through self-assembling monolayers, polycation layering, sol–gel and conducting polymers, clay colloids, or carbon paste, all of which provide electron-conducting pathways between the protein and the electrode [35–42]. The relatively low amperometric detection limit obtained for L-cysteine–HRP–SWNTs-modified electrode is lower than the 2.5×10^{-7} M reported for HRP immobilized in ZrO_2-Grafted Collagen/DMSO Membranes [43], 1×10^{-7} M for HRP–CPE incorporating the graphite powder [44], and 2.5×10^{-7} M for HRP-Chi-BMIM·BF4/GC electrode [45]. Recently, a method to determine hydrogen peroxide in macrophage RAW 264.7 cell extracts with the detection limit of 5.6 nM were reported [46].

Hydrogen peroxide which present in aerobic cells as a metabolite in low concentrations is generated by nonenzymatic and superoxide dismutase-catalyzed dismutation reactions. The active oxygen species H_2O_2, superoxide anion and hydroxyl radical have been implicated as a cause of cellular death [47]. H_2O_2 causes DNA single-strand break in human fibroblasts. Thus, the method to determine H_2O_2 of low concentration is desired for constructing. In the present study, by combining the advantageous features of SWNTs and S–Au, a novel H_2O_2 biosensor has been constructed. The advantages of L-cysteine–HRP–SWNTs-modified gold electrode are the low detection limit and the high activity of HRP. We have developed a hydrogen peroxide biosensor, in which horseradish peroxidase was immobilized onto a functionalized SWNT through noncovalent method and the carboxylic groups of the functionalized SWNT was immobilized onto an amino-terminated L-cysteine self-assembled monolayer (SAM) performed on the Au electrode. The low detection limit obtained in this work is attributed to the intimate contact resulting from the close proximity between enzyme and electrode, attached by SWNTs.

2. Experimental

2.1. Materials

Single-walled carbon nanotubes were purchased from Nanoport. Co. Ltd. (Shenzhen, China). Horseradish peroxidase (HRP) was obtained from Sigma. L-Cysteine, sodium cholate, N-(3-dimethylamino)propyl-N-ethylcarbodiimide hydrochloride (EDC) and N-hydroxysulfosuccinimide (NHS) were purchased from Aldrich. A phosphate buffer saline solution (PBS) was prepared by modifyng 0.01 M disodium hydrogen phosphate (Aldrich) with the admixture of 0.01 M sodium dihydrogen phosphate (Aldrich) with 0.1 M sodium chloride. All other reagents used were of analytical reagent grade. Deionized water was used throughout to prepare all solutions, and a high purity nitrogen atmosphere was maintained in the cell during the whole period of experiments.

2.2. Apparatus

2.2.1. Electrochemical measurements

Electrochemical experiments were carried out using a CHI 660 (CH Instruments Co. Ltd., Austin, USA) with a three-electrode cell. The gold (or modified gold) electrode, a platinum wire, and saturated calomel electrode (SCE) were used as working, counter and reference electrode, respectively.

2.2.2. UV–vis spectrophotometry

To monitor the biosensor, we assembled L-cysteine–HRP–SWNTs and L–cysteine–SWNTs on ITO substrates deposited gold nanopaticles. Absorption spectra were taken with a UV-1102 vis spectrophotomer (Tianmei Science Instruments Co. Ltd., Shanghai, China) of films fabricated with HRP.

Scanning electron microscope (SEM) measurements. Surface images of the L–cysteine-modified gold film before and after integrating the HRP–SWNTs were obtained by SEM (JSM-6701F, Electron Optics Co., Japan) measurement.

2.3. Preparation of enzyme electrodes

2.3.1. Purification and oxidation of SWNTs (Fig. 1a)

Hydrogen peroxide (30%, 50 ml) was measured into a graduated cylinder followed by careful addition of concentrated hydrochloric acid (36%, 50 ml). The acid mixture was slowly added to the flask containing with SWNTs (100 mg), and the mixture was sonicated for 6 h. The resulting nanotubes were then filtered through a PTFE 0.2 μm membrane and washed with deionized water to neutral pH.

2.3.2. Adsorption of enzyme to SWNTs (Fig. 1b)

Highly dispersed and debundled SWNTs were prepared by the sodium cholate suspension-dialysis method [8,9]. In this method SWNTs were first debundled with the bile salt sodium cholate, the adsorbed cholate was subsequently replaced by horseradish peroxidase (HRP), and the sodium cholate was removed by dialysis. Initially, a saturated suspension of single-wall carbon nanotubes (SWNTs) was made by first adding 3 mg of SWNTs with carboxylic groups to 7 ml of a 2 wt% aqueous solution of sodium cholate. Next, the mixture was sonicated for 1 h using a homogenizer (22% amplitude, Cole-Parmer model CPX750) resulting in a dark black liquid. Then, the SWNTs solution was centrifuged at $30{,}100 \times g$ for 1 h at temperature 4 °C, and the supernatant was retained. Sodium phosphate was added to 5 ml of supernatant SWNTs solution to give a concentration of 20 mM. Next 20 mg of HRP was added to the SWNTs solution and mixed well. The sodium cholate that was displaced as the HRP adsorbed onto the SWNTs was removed by dialysis with a 10 KDa dialysis membrane (Spectrum Laboratories) and 1.5 L of a 20 mM phosphate buffer (pH 7.5) for 12 h at 4 °C. Next the resulting HRP–SWNT solution was transferred to a 100 kDa dialysis membrane (Spectrum Laboratories) and dialyzed at 4 °C to remove any unabsorbed HRP, with a change of the buffer frequently. The final suspension was centrifuged at $29{,}600 \times g$ for 1 h and the supernatant was retained.

2.3.3. Self-assembled L-cysteine on gold electrode (Fig. 1c)

The Au disk electrode (diameter 3.0 mm) was polished with 0.3, and 0.05 μm alumina powders consecutively to get a mirror-like surface and then sonicated in deionized water for 5 min. Prior to use, the electrode was electrochemically pretreated by cycling the potential from −0.2 to +1.6 V in 0.5 M H_2SO_4 solution at the scan rate of $0.10\,V\,s^{-1}$ to get a stable voltammogram. Modification by

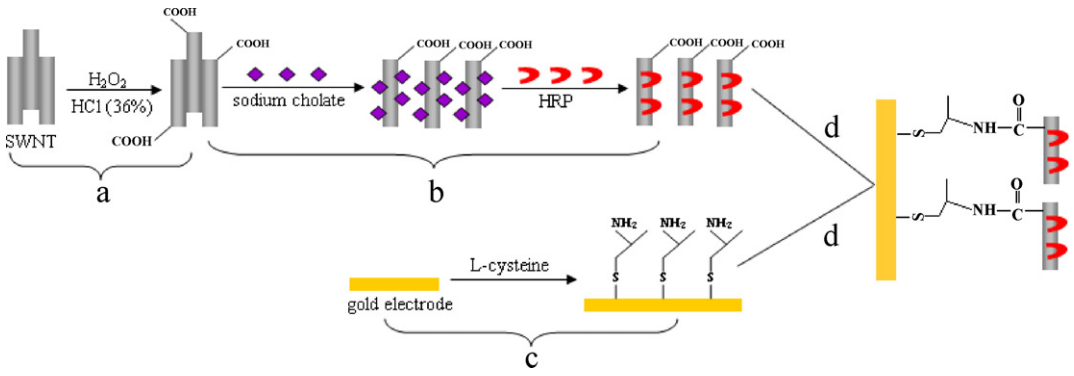

Fig. 1. Schematic of preparation of enzyme electrodes.

L-cysteine was accomplished by immersing the well pretreated gold disk electrode in 0.01 M L-cysteine for 4 h. Then, the treated electrode was rinsed with deionized water.

2.3.4. Construction of the enzyme electrodes (Fig. 1d)

N-(3-dimethylamino)propyl-N-ethylcarbodiimide hydrochloride (EDC) and N-hydroxysulfosuccinimide (NHS) as a coupling agent was added in 1 ml of HRP–SWNTs for 45 min. Then the coupling agent unused was removed by dialysis. The enzyme electrode was accomplished by immersing the modified gold electrode in the HRP–SWNTs treated with EDC and NHS for 48 h.

3. Results and discussion

3.1. Characterization of the L-cysteine–HRP–SWNTs-modified gold film

SEM is a powerful tool to characterize the morphologies of different composites. Fig. 2 shows the SEM images of the L-cysteine-modified gold film before (Fig. 2a) and after integrating the HRP–SWNTs (Fig. 2b). After the covalence of the HRP–SWNTs (Fig. 2b), SWNTs were seen to be distributed on the surface of L-cysteine-modified gold film and some of them intercalated into the interior film.

3.2. Electrochemical characteristics of the modified electrode

Cyclic voltammetry (CV) is especially well-suited to study of electron-transfer kinetics of electroactive species. Fig. 3 shows the cyclic voltammograms of different electrodes in 0.01 M pH 7.0 PBS. The L-cysteine–HRP–SWNTs-modified electrode gives a couple of stable and well-defined redox peaks at −0.203 and −0.394 V at 0.05 V s^{-1} (curve d in Fig. 3), while no redox peak is observable at the bare gold electrode (curve a in Fig. 3), L-cysteine-modified electrode (curve b in Fig. 3) and L-cysteine–SWNTs-modified electrode (curve c in Fig. 3). Obviously, the response of the L–cysteine–HRP–SWNTs-modified electrode is attributed to the redox of the electroactive centers in the HRP.

The cyclic voltammograms of the L-cysteine–HRP–SWNTs-modified electrode displays a well-defined peak shape at different scan rates (Fig. 4). Cathodic peak currents vary linearly with the scan rates, as shown in the inset of Fig. 4, indicating a surface-controlled electrode process.

3.3. UV–vis characterizations

HRP contains heme as a prosthetic group, which is also the protein active site, and it can catalyze the hydrogen peroxide-dependent one-electron oxidation of a wide variety of substrates. UV–vis spectroscopy is an effective means for monitoring the possible change of the Soret absorption band in the heme group region. The band shift may provide information on the tertiary structure of HRP, especially that conformational change around the active site of the HRP [45,48]. Fig. 5 shows the spectra of HRP in PBS solution of pH 7.5 (curve a) and L-cysteine–HRP–SWNTs assembled layers on ITO glass deposited gold nanopaticles (curve b). For HRP in PBS, the Soret band lies at 402 nm, while it is shifted to 408 nm in the L-cysteine–HRP–SWNTs assembled film. The slight shift in the Soret band and the decrease in its absorbance may be due to the interaction between SWNTs and proteins for the surface potential energy and adsorption [26]. Such interactions neither destroy

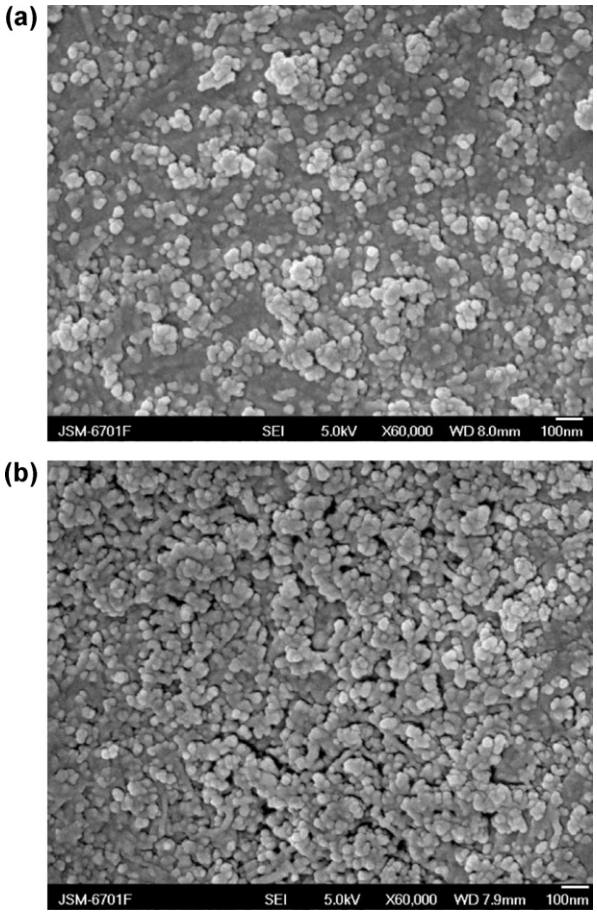

Fig. 2. SEM images of the films. (a) L-Cysteine-modified gold film. (b) L-Cysteine–HRP–SWNTs-modified gold film.

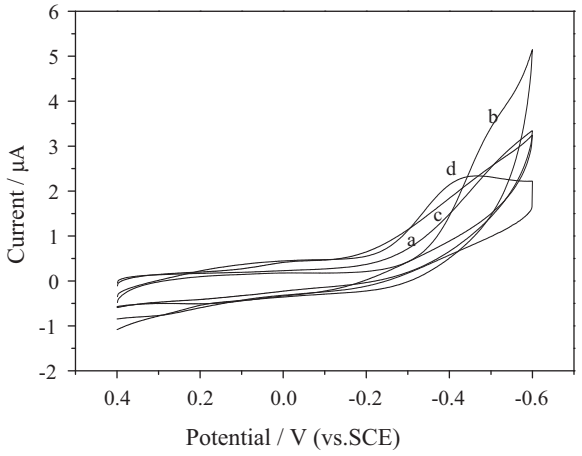

Fig. 3. Cyclic voltammograms of the electrodes at different stages: (a) bare gold electrode, (b) L-cysteine-modified electrode, (c) L-cysteine-SWNTs-modified electrode, and (d) L-cysteine–HRP–SWNTs-modified electrode. The curves were obtained in 0.01 M PBS (pH 7.5) and scan rate 50 mV s^{-1}.

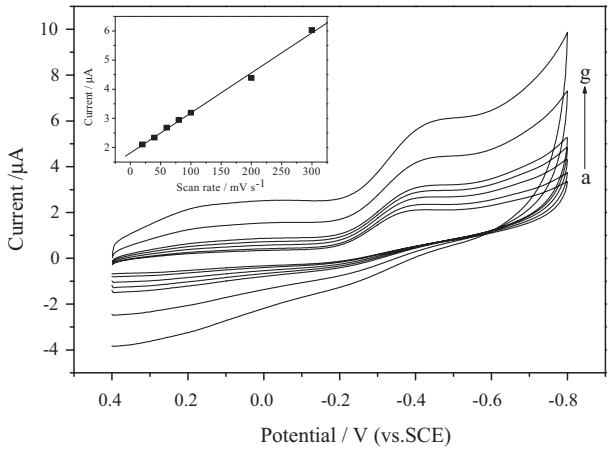

Fig. 4. Cyclic voltammograms of the L-cysteine–HRP–SWNTs-modified electrode in 0.01 M pH 7.5 PBS at different scan rates. The scan rates form inner to outer are (a) 20, (b) 40, (c) 60, (d) 80, (e) 100, (f) 200, and (g) 300 mV s^{-1}. Inset: The plot of cathodic peak currents vs. scan rates.

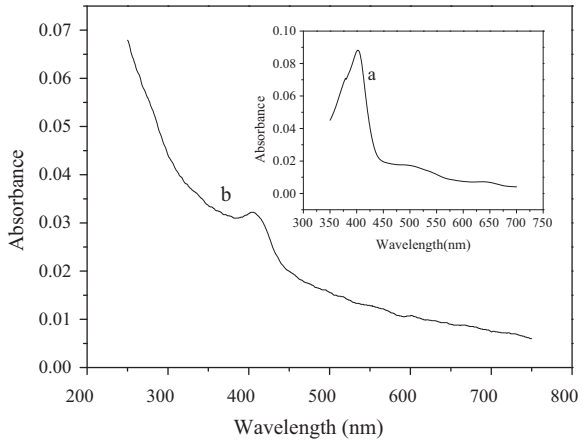

Fig. 5. UV–vis spectra for (a) HRP in PBS (pH 7.5) and (b) L-cysteine–HRP–SWNTs assembled layers on ITO glass deposited gold nanopaticles.

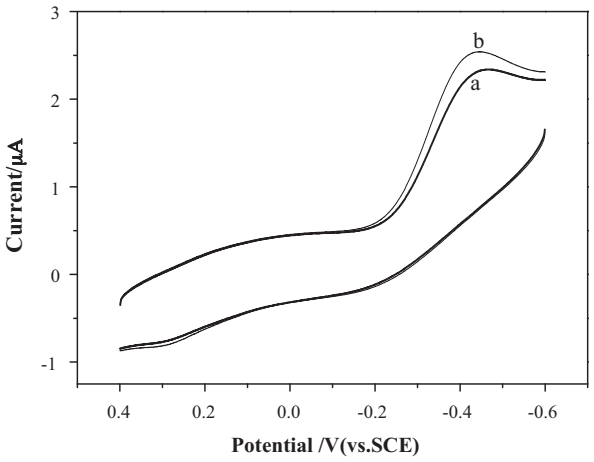

Fig. 6. Linear sweep voltammograms of the biosensor in PBS pH 7.5 without (a) and with 3.0×10^{-12} M H_2O_2. (b) Scan rate 50 mV s^{-1}.

the structure nor change the fundamental microenvironment of the biomolecules.

3.4. Linear sweep voltammetric response of biosensor to H_2O_2

The electrocatalytic reactivity of the L-cysteine–HRP–SWNTs electrode toward H_2O_2 is investigated by linear sweep voltammetry (LSV). Fig. 6 depicts the electrocatalytic response of the electrode in pH 7.5 PBS with and without the presence of H_2O_2. A pair of oxidation–reduction peak is observed in the blank PBS (Fig. 6, curve a), which contributes to the redox reaction of HRP. Upon the addition of 3×10^{-12} M H_2O_2 in the substrate solution, the reduction peak current increases obviously from 2.36 to 2.55 μA, while the oxidation current has no change (Fig. 6, curve b), suggesting a typical electrocatalytic reduction process of H_2O_2. Good electrocatalytic activity of the modified electrode for H_2O_2 is attributed to the presence of SWNTs and HRP. This result indicates that the SWNTs could effectively shuttle electrons from the base electrode surface to the redox center of HRP.

3.5. Effect of pH on the biosensor response

It is known that pH influences the conformation of the enzyme and its bioactivity, which is studied by measuring the current response to PBS of 0.01 M in the pH range of 6.0–9.0. Fig. 7 shows that HRP of this biosensor exhibit best activity in the solution of pH

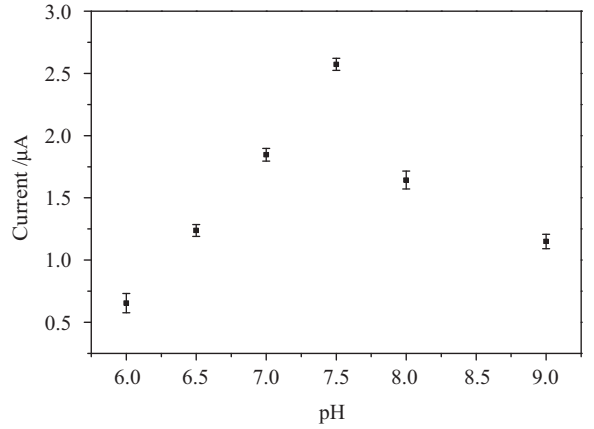

Fig. 7. Effect of PBS pH on the electrocatalytic responses of the L-cysteine–HRP–SWNTs-modified electrode. Error bar = ±S.D. and $n = 3$.

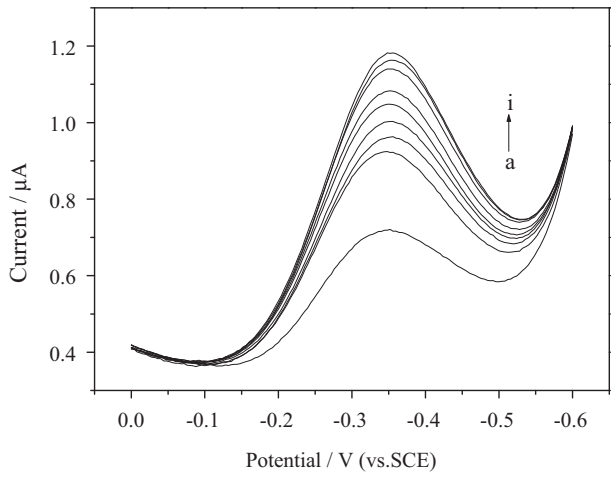

Fig. 8. Differential pulse voltammograms of the L-cysteine–HRP–SWNTs-modified electrode in 0.01 M pH 7.5 PBS containing (a) 0, (b) 1, (c) 3, (d) 5, (e) 7, (f) 9, (g) 30, (h) 50, and (i) 70×10^{-12} M H_2O_2.

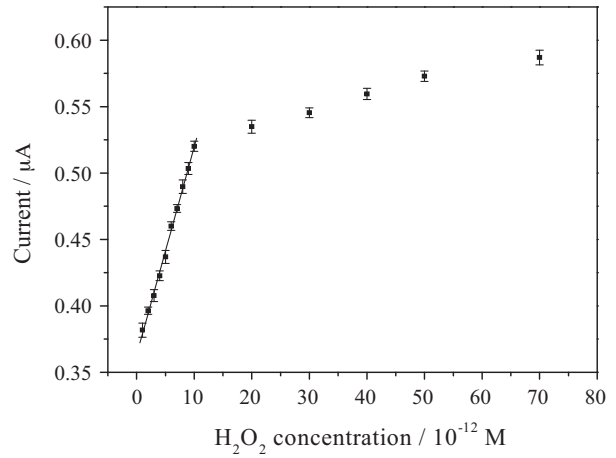

Fig. 9. Relationship between the concentration of H_2O_2 and response current. Error bar = ±S.D. and $n = 3$.

7.5, it may be due to the adsorbed HRP that it maintains its higher bioactivity at such a pH. It is observed that the sensor response is significantly deteriorated after being exposed to buffers of pH values smaller than 7.0 or greater than 8.0.

3.6. Amperometric response and calibration curve

Fig. 8 shows the dynamic amperometric response of the modified electrodes, characterized by a well bioelectrocatalytic response for H_2O_2. Fig. 9 shows the corresponding calibration curve between amperometric current and H_2O_2 concentration. The linear response range is from 1.0×10^{-12} to 1.0×10^{-11} M with a correlation coefficient of 0.9986 and a detection limit of 2.1×10^{-13} M at a signal-to-noise ratio of 3.

4. Conclusion

In this study, we demonstrate that HRP–SWNTs conjugates produced by the sodium cholate suspension-dialysis method were highly dispersed and retained a significant amount of native enzymatic activity. We also demonstrate that these HRP–SWNT conjugates can be combined with L-cysteine assembled on the gold electrode by the self-assembly technique to fabricate highly sensitive sensors to H_2O_2. HRP–SWNTs were constructed in order to improve the enzyme immobilization on the substrate. A most significant aspect of this work is the high biocatalytic response of the sensors, and the detection limit is lowest ever reported biosensors based on HRP. A second important aspect of this work is that this method may serve as a model to improve the quality of many other analytical biodevices and allow for miniaturization in biosensor development and for increased power output in biofuel cell applications. Future generations of arrayed electrochemical sensors and studies of direct electron transfer of enzymes can benefit from protein electrodes prepared by this method.

Acknowledgments

This work was supported by the Natural Science Foundation of China (Nos. 21175108, 20875077 and 20927004), the Natural Science Foundation of Gansu (No. 0701RJZA109) and Key Laboratory of Polymer Materials of Gansu Province, China.

References

[1] A. Heller, Acc. Chem. Res. 23 (1990) 128–134.
[2] C.E. Banks, T.J. Davies, G.G. Wildgoose, R.G. Compton, Chem. Commun. 7 (2005) 829–841.
[3] M. Musameh, J. Wang, A. Merkoci, Y. Lin, Electrochem. Commun. 7 (2002) 744–745.
[4] L. Wu, X. Zhang, H. Ju, Anal. Chem. 79 (2007) 453–458.
[5] M. Zhou, J. Ding, L.P. Guo, Q.k. Shang, Anal. Chem. 79 (2007) 5328–5335.
[6] M. Zhou, J. Guo, L.P. Guo, J. Bai, Anal. Chem. 80 (2008) 4642–4650.
[7] B. Eric, Q. Yu, Anal. Chem. 78 (2006) 3965–3984.
[8] S. Iijima, T. Ichihashi, Nature 363 (1993) 603–605.
[9] M.L. Usrey, E.S. Lippmann, M.S. Strano, J. Am. Chem. Soc. 127 (2007) 16129–16135.
[10] Y. Mao, S. Banerjee, S.S. Wong, Electrochem. Commun. 3 (2003) 408–409.
[11] Y. Yan, W. Zheng, M. Zhang, L. Wang, L. Su, L. Mao, Langmuir 21 (2005) 6560–6566.
[12] A. Thess, R. Lee, P. Nikolaev, H.J. Dai, P. Petit, J. Robert, C.H. Xu, Y.H. Lee, S.G. Kim, A.G. Rinzler, D.T. Colbert, G.E. Scuseria, D. Tomanek, J.E. Fischer, R.E. Smalley, Science 273 (1996) 483–487.
[13] T. Tsai, G. Heckert, L.F. Neves, Y. Tan, D. Kao, R.G. Harrison, D.E. Resasco, D.W. Schmidtke, Anal. Chem. 81 (2009) 7917–7925.
[14] N.R. Palwai, D.E. Martyn, L.F.F. Neves, Y. Tan, D.E. Resasco, R.G. Harrison, Nanotechnology 18 (2007) 235601.
[15] S. Attal, R. Thiruvengadathan, O. Regev, Anal. Chem. 78 (2006) 8098–8104.
[16] M.E.G. Lyons, G.P. Keeley, Chem. Commun. 22 (2008) 2529–2531.
[17] M.E.G. Lyons, G.P. Keeley, Sensors 6 (2006) 1791–1826.
[18] M.E.G. Lyons, G.P. Keeley, Int. J. Electrochem. Sci. 3 (2008) 819–853.
[19] P. Asuri, S.S. Karajanagi, R.S. Kane, J.S. Dordick, Small 3 (2007) 50–53.
[20] J.L. Bahr, J.M. Tour, J. Mater. Chem. 12 (2002) 1952–1958.
[21] F. Buffa, H. Hu, D.E. Resasco, Macromolecules 38 (2005) 8258–8263.
[22] M.S. Strano, C.A. Dyke, M.L. Usrey, P.W. Barone, M.J. Allen, H. Shan, C. Kittrell, R.H. Hauge, J.M. Tour, R.E. Smalley, Science 301 (2003) 1519–1522.
[23] D. Nepal, K.E. Geckeler, Small 2 (2006) 406–412.
[24] P.W. Barone, S. Baik, D.A. Heller, M.S. Strano, Nat. Mater. 4 (2005) 86–92.
[25] R.J. Chen, Y. Zhang, D. Wang, H. Dai, J. Am. Chem. Soc. 123 (2001) 3838–3839.
[26] D. Shan, E. Han, H. Xue, S. Cosnier, Biomacromolecules 8 (2007) 3041–3046.
[27] R.G. Nuzzo, D.L. Allara, J. Am. Chem. Soc. 105 (1983) 4481–4483.
[28] J. Shi, X. Zhang, W. Xie, Y. Zhou, Z. Zhang, J. Deng, A.E.G. Cass, Z. Zhang, D. Pang, C. Zhang, Anal. Chem. 76 (2004) 632–638.
[29] A.C. Templeton, W.P. Wuelfing, R.W. Murray, Acc. Chem. Res. 33 (2000) 27–36.
[30] R.G. Nuzzo, L.H. Dubois, D.L. Allara, J. Am. Chem. Soc. 112 (1990) 558–569.
[31] Y.L. Zhou, N.F. Hu, Y.H. Zeng, J.F. Rusling, Langmuir 18 (2002) 211–219.
[32] Y. Tian, L. Mao, T. Okajima, T. Ohsaka, Anal. Chem. 74 (2002) 2428–2434.
[33] C.H. Fan, H.Y. Wang, S. Sun, D.X. Zhu, G. Wagner, G.X. Li, Anal. Chem. 73 (2000) 2850.
[34] Z. Dai, F. Yan, J. Chen, H. Ju, Anal. Chem. 75 (2003) 5429–5434.
[35] R. Polsky, J.C. Harper, S.M. Dirk, D.C. Arango, D.R. Wheeler, S.M. Brozik, Langmuir 23 (2007) 364.
[36] Y. Xiao, F. Patolsky, E. Katz, J.F. Hainfeld, I. Willner, Science 299 (2003) 1877–1881.
[37] J.J. Gooding, F. Mearns, W. Yang, J. Liu, Electroanalysis 15 (2003) 81–96.
[38] H. Ma, N. Hu, J.F. Rusling, Langmuir 16 (2000) 4969–4975.
[39] T.J. Ohara, R. Rajagopalan, A. Heller, Anal. Chem. 66 (1994) 2451–2457.

[40] W. Schuhmann, Mikrochim. Acta 121 (1995) 1–29.
[41] Y. Zhou, N. Hu, Y. Zeng, J.F. Rusling, Langmuir 18 (2002) 211–219.
[42] L. Gorton, Electroanalysis 7 (1995) 23–45.
[43] S. Zong, Y. Cao, Y. Zhou, H. Ju, Langmuir 22 (2006) 8915–8919.
[44] I.C. Popescu, G. Zetterberg, L. Gorton, Biosen. Bioelectron. 10 (1995) 443–461.
[45] X. Lu, Q. Zhang, L. Zhang, J. Li, Electrochem. Commun. 8 (2006) 874–878.
[46] H. Li, Q. Li, X. Wang, K. Xu, Z. Chen, X. Gong, X. Liu, L. Tong, B. Tang, Anal. Chem. 81 (2009) 2193–2198.
[47] A.C. Mello Filho, M.E. HOffmanntt, R. Meneghini, Biochem. J. 218 (1984) 273–275.
[48] P. George, G. Hanania, J. Biochem. 55 (1953) 236–243.